

# Effect of annealing on the structural and electrical properties of $\text{In}_2\text{Te}_3$

N. A. HEGAB, M. A. AFIFI, A. E. EL-SHAZLY, A. E. BEKHEET

*Physics Department, Faculty of Education, Ain Shams University, Cairo, Egypt*

Amorphous  $\text{In}_2\text{Te}_3$  was prepared in both bulk form, by quenching the molten material, and thin-film form, by the thermal evaporation technique. X-ray diffraction analysis showed that the prepared samples in bulk and as-deposited thin-film forms were in the amorphous state.  $\beta$ - and  $\alpha$ -phases of  $\text{In}_2\text{Te}_3$  were prepared by annealing bulk samples at 615 and 813 K, respectively. Films annealed at 573 K give  $\beta$ -phase polycrystalline structure. The electrical conductivity for the as-deposited  $\text{In}_2\text{Te}_3$  films increases with increasing film thickness. The conduction activation energy,  $\Delta E_\sigma$ , of the as-prepared bulk and thin film samples were found to be 0.516 and 0.521 eV. The corresponding values of room-temperature electrical conductivity,  $\sigma_{\text{RT}}$ , for these samples are  $1.1 \times 10^{-6}$  and  $7.15 \times 10^{-7} \Omega^{-1} \text{m}^{-1}$ , respectively. The observed change in the value of  $\sigma_{\text{RT}}$  may be due to the difference in the structure of bulk and thin-film samples. The increase of  $\Delta E_\sigma$  with annealing temperature for both bulk and thin-film samples is interpreted in terms of the density of states model proposed by Mott and Davis. © 1998 Chapman & Hall

## 1. Introduction

According to the phase diagram given by Grochowski *et al.* [1], it is obvious that three compounds in the In–Te system,  $\text{In}_2\text{Te}_3$ , InTe and  $\text{In}_4\text{Te}_7$ , are stable.  $\text{In}_2\text{Te}_3$ , a member of this family, has very interesting electrical and optical properties [2–6] for an eventual use in solar cells or detectors. X-ray studies have shown that it crystallizes in two polymorphic modifications  $\alpha$ - and  $\beta$ - $\text{In}_2\text{Te}_3$  [7–10].  $\beta$ -phase  $\text{In}_2\text{Te}_3$  has a zincblende structure [11] which is characterized by a completely random distribution of the metal ions in their sublattice. It can be transformed to the ordered state (the  $\alpha$ -phase) as obtained by Kosevich *et al.* [12] via their study of the effect of annealing with an electron beam on the structure of amorphous  $\text{In}_2\text{Te}_3$  films. On increasing the intensity of the electron beam, amorphous  $\text{In}_2\text{Te}_3$  was transformed to hexagonal  $\text{In}_2\text{Te}_3$  ( $\beta$ -phase), then to cubic  $\text{In}_2\text{Te}_3$  ( $\alpha$ -phase) and finally to InTe. Zahab *et al.* [3] have shown that an appropriate annealing of  $\text{In}_2\text{Te}_3$  films leads to a polycrystalline  $\beta$ - $\text{In}_2\text{Te}_3$  with a preferred orientation in the [1 1 1] direction.

In this work, the structural and electrical properties of  $\text{In}_2\text{Te}_3$  in both bulk and thin film forms were studied. The effect of annealing at different temperatures on the structural and electrical properties of  $\text{In}_2\text{Te}_3$  was also investigated.

## 2. Experimental procedure

Amorphous  $\text{In}_2\text{Te}_3$  was synthesized [13] by direct fusion of stoichiometric amounts of indium and tellurium (purity 99.999%) in an evacuated sealed silica

tube ( $10^{-5}$  torr; 1 torr = 133.322 Pa). The temperature of the tube was raised at a rate of  $50 \text{ K h}^{-1}$  to 1073 K at which it was kept constant for 3 days, then quenched in icy water. X-ray diffraction analysis and differential thermal analysis (DTA) revealed the amorphous nature of the structure of the investigated compound. Thin-film samples of the synthesized amorphous  $\text{In}_2\text{Te}_3$  were obtained by thermal evaporation technique under vacuum on to glass substrates whose temperature was kept constant at room temperature. The film thickness was controlled during deposition using a thickness monitor (Edward FTM5) and was measured after deposition by Tolansky's interferometric method [14]. The chemical composition of the obtained films was checked by energy dispersive X-ray analysis (EDX) using a scanning electron microscope (Joel 5400). Electrical conductivity for  $\text{In}_2\text{Te}_3$  in bulk and thin-film forms was measured by the two-probe method using a specially constructed sample holder, shown in Fig. 1a and b, for each type of sample. A Keithely electrometer (616A) was used to measure the electrical resistance of the as-prepared samples and of samples after annealing at different temperatures.

## 3. Results and discussion

### 3.1. Structural identification of $\text{In}_2\text{Te}_3$ in bulk form

Fig. 2 shows a DTA thermogram of amorphous  $\text{In}_2\text{Te}_3$  in bulk form. An initial plateau can be seen extending to about 437 K, followed by an endothermic peak at 443 K which corresponds to the glass

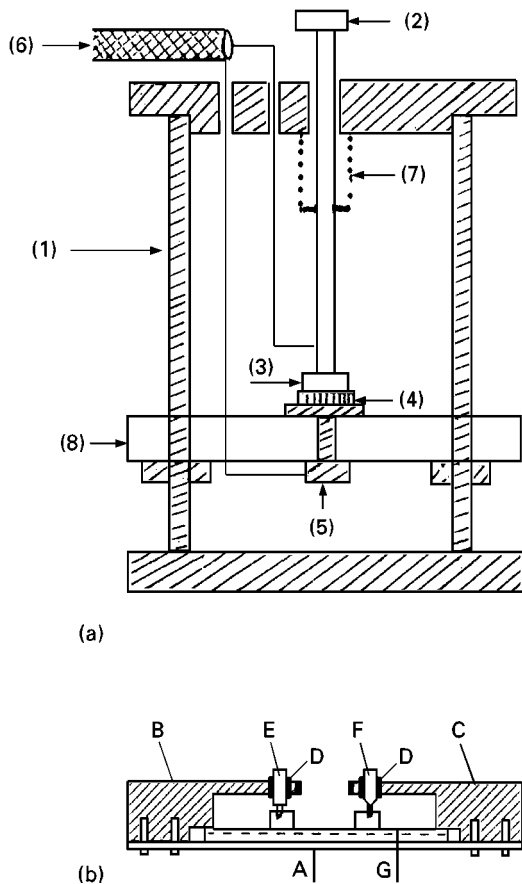


Figure 1 Schematic representation of the cell used for conductivity measurements for (a) bulk samples, and (b) thin-film samples. (a) 1, Brass body holder; 2, movable upper electrode; 3, connecting end of the upper electrode; 4, specimen; 5, lower electrode; 6, shielded cable; 7, spring resting on a fixed transverse. (b) A, Flat rectangular brass sheet; B, C two brass arms; E, F, two small pistons; D, a teflon cup.

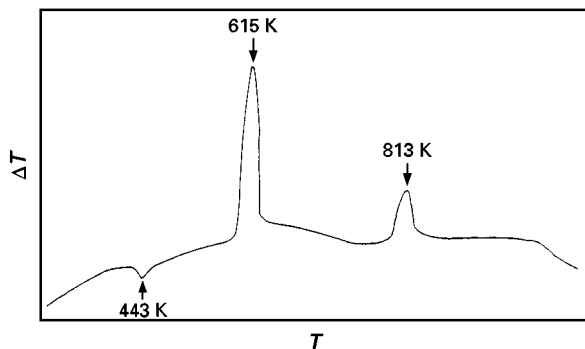


Figure 2 Differential thermal analysis of the as-prepared  $\text{In}_2\text{Te}_3$  in powder form.

transition temperature,  $T_g$ , of the investigated compound. Then two exothermic peaks began at 583 and 793 K with maximum values at 615 and 813 K, respectively. The first peak may correspond to the crystallization temperature,  $T_c$ , of the amorphous material into the  $\beta$ -phase, while the second may correspond to the phase transformation from  $\beta$ - to  $\alpha$ - $\text{In}_2\text{Te}_3$  phase. To confirm these results, two samples were annealed under vacuum for 24 h at 615 and 813 K, respectively. Fig. 3 shows X-ray patterns for the annealed samples together with that of the as-prepared sample. It is clear

from the figure that the annealed samples have a polycrystalline structure. Careful analysis of the results of indexing the pattern of the sample annealed at 813 K, together with JCPDS card 16-445, indicates a polycrystalline nature for the cubic structure called  $\alpha$ -phase. The result of indexing the pattern of the sample annealed at 615 K is found to be consistent with these reported before [15, 16] for  $\beta$ - $\text{In}_2\text{Te}_3$ . The obtained X-ray results are in harmony with the above DTA results.

### 3.2. Structural identification of $\text{In}_2\text{Te}_3$ films

X-ray diffraction patterns obtained for the as-deposited  $\text{In}_2\text{Te}_3$  film indicate that it has amorphous structure, as shown in Fig. 4a. To investigate the effect of annealing temperature on the structure of  $\text{In}_2\text{Te}_3$  samples, films of different thicknesses were annealed under vacuum for 4 h at 473, 523 and 573 K. X-ray diffraction patterns of the annealed films are shown in Fig. 4b, c and d. It is clear that  $\text{In}_2\text{Te}_3$  films annealed at temperatures less than or equal to 523 K still have an amorphous structure, while those annealed at 573 K have polycrystalline structure. The result of indexing the pattern of the polycrystalline sample are found to be quite consistent with those reported before [15, 16] for  $\beta$ - $\text{In}_2\text{Te}_3$  crystals.

### 3.3. Electrical properties of $\text{In}_2\text{Te}_3$ in the bulk form

The temperature dependence of electrical conductivity  $\sigma$ , was studied for the as-prepared and the annealed  $\text{In}_2\text{Te}_3$  samples in the bulk form in the temperature range 298–423 K. The results obtained during heating–cooling cycles are illustrated in Fig. 5. It is clear from the figure that the heating–cooling cycles coincide with each other in the investigated temperature range. The activation energy was calculated for the investigated samples from the slopes of the straight lines of Fig. 5 and using the equation

$$\sigma = \sigma_0 \exp(-\Delta E_\sigma/kT) \quad (1)$$

where  $\Delta E_\sigma$  is the electrical conduction activation energy,  $\sigma_0$  the pre-exponential factor,  $k$  Boltzmann's constant and  $T$  the temperature in Kelvin. The calculated values of  $\Delta E_\sigma$  are 0.516, 0.571 and 0.575 eV for amorphous,  $\beta$ -phase and  $\alpha$ -phase, respectively. The obtained values of  $\Delta E_\sigma$  are in agreement with those obtained previously by Hussein and Nagat [2] and Sen and Bose [6] for  $\text{In}_2\text{Te}_3$  single crystal which are 0.53 and 0.55 eV, respectively.

### 3.4. Electrical properties of the as-deposited $\text{In}_2\text{Te}_3$ films

#### 3.4.1. Thickness dependence of electrical conductivity

The thickness dependence of the room-temperature electrical conductivity,  $\sigma_{RT}$ , of the as-deposited  $\text{In}_2\text{Te}_3$  films studied in the thickness range 50–620 nm, is shown in Fig. 6. It is clear from the figure that

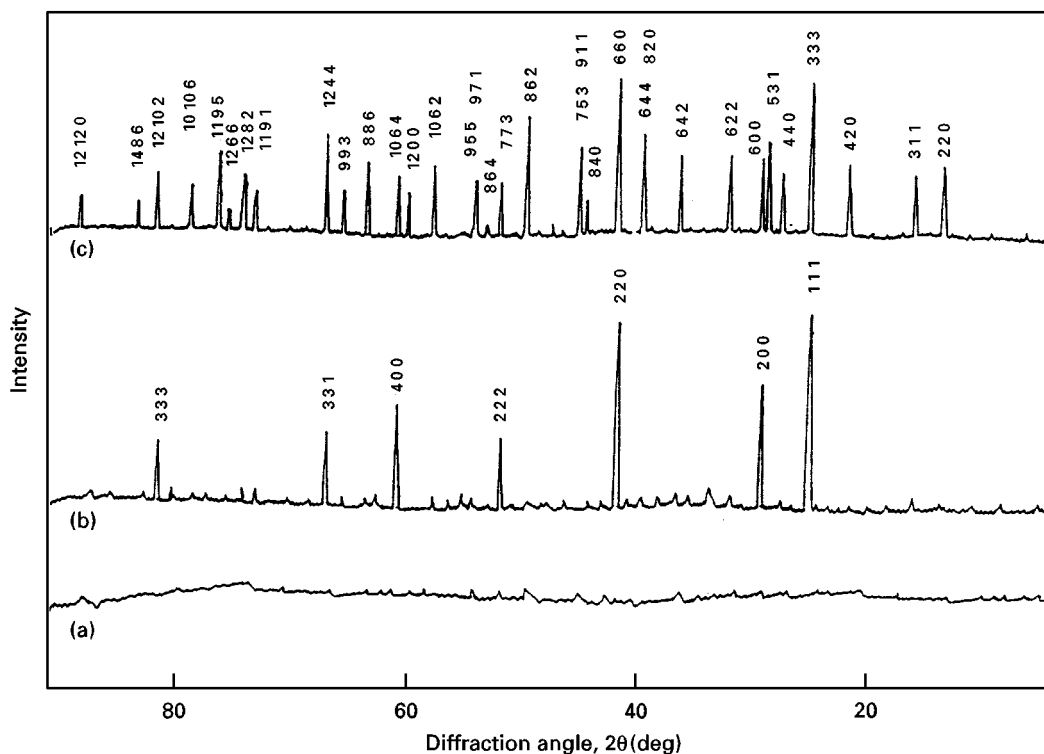


Figure 3 X-ray diffraction of In<sub>2</sub>Te<sub>3</sub> in bulk form. (a) as-prepared, (b) annealed at 615 K, (c) annealed at 813 K.

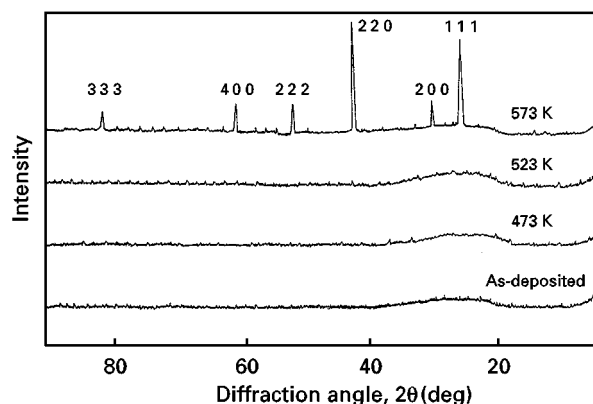


Figure 4 X-ray diffraction of In<sub>2</sub>Te<sub>3</sub> films annealed at different temperatures.

$\sigma_{RT}$  seems to increase exponentially with increasing thickness and tends to be constant for films of thickness greater than 392 nm. This behaviour can be attributed to lattice defects, such as vacancies, interstitials and dislocations which might be distributed throughout the first stages of film growth. The defects add an extra percentage of resistivity. Because the defects diffuse, the corresponding resistivity thus decreases and hence conductivity increases as the film thickness increases.

### 3.4.2. Temperature dependence of electrical conductivity

The temperature dependence of electrical conductivity,  $\sigma$ , was studied for the as-deposited In<sub>2</sub>Te<sub>3</sub> films of different thicknesses greater than 392 nm in the temperature range 298–423 K during heating-cooling

cycles. It must be noticed that the investigated range of thickness (392–620 nm) is the range in which  $\sigma$  is independent of thickness. The obtained data for a film of thickness 492 nm is shown in Fig. 7 as a representative example. It is clear from the figure that the heating-cooling cycles coincide with each other in the investigated temperature range. Fig. 8 shows the above-mentioned conductivity variations during heating only for In<sub>2</sub>Te<sub>3</sub> films of different thicknesses. It is clear from the figure that there is no marked difference between these films, which means that  $\sigma$  and  $\Delta E_{\sigma}$  are independent of the thickness of the film in the investigated range. Value of  $\Delta E_{\sigma}$  was found to be 0.521 eV. Values of  $\sigma_{RT}$  for bulk and thin-film forms are  $1.1 \times 10^{-6}$  and  $7.15 \times 10^{-7} \Omega^{-1} \text{m}^{-1}$ , respectively.

To investigate the observed changes in electrical conductivity between bulk and thin-film samples, the sample composition was studied by energy dispersive X-ray spectroscopy (EDX). The composition of the films is found to be essentially the same as that in the bulk. Furthermore, the thickness independence of the electrical conductivity,  $\sigma$ , in the investigated range indicates that the change between film and bulk samples cannot be caused by any surface effect or absorption effect. So these changes may be due to the difference in the network structure of samples.

The obtained value  $\Delta E_{\sigma}$  (0.521 eV) for amorphous films is half that obtained before [17] for the value of the optical gap (1.02 eV) which is in good agreement with the results of most amorphous semiconductors.

### 3.4.3. Effect of annealing

To investigate the effect of annealing on the room-temperature electrical conductivity,  $\sigma_{RT}$ , four samples

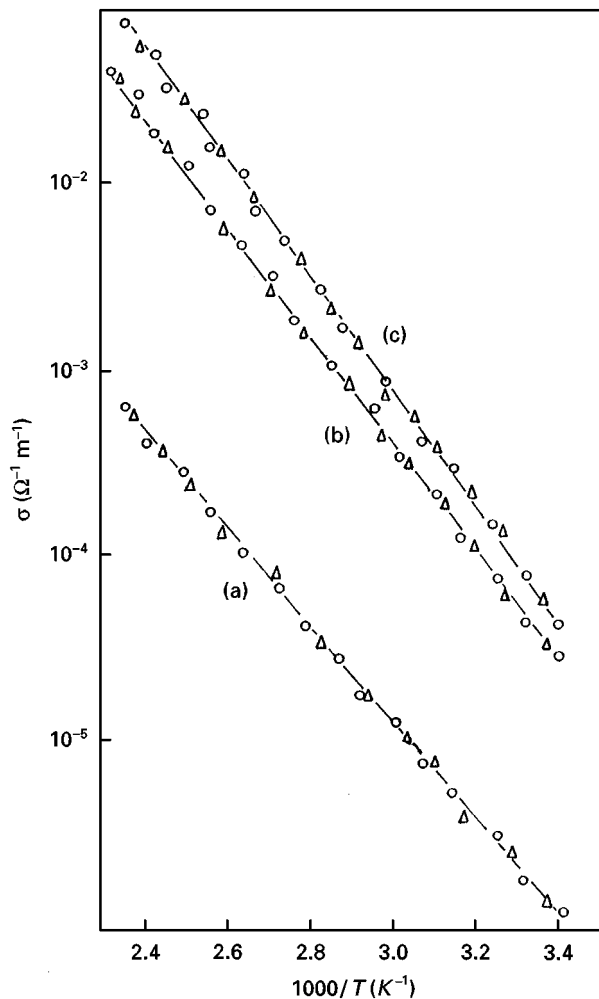


Figure 5 Temperature dependence of electrical conductivity for  $\text{In}_2\text{Te}_3$  in bulk form on (○) heating, and (△) on cooling. (a) Amorphous, (b)  $\beta$ -phase, (c)  $\alpha$ -phase.

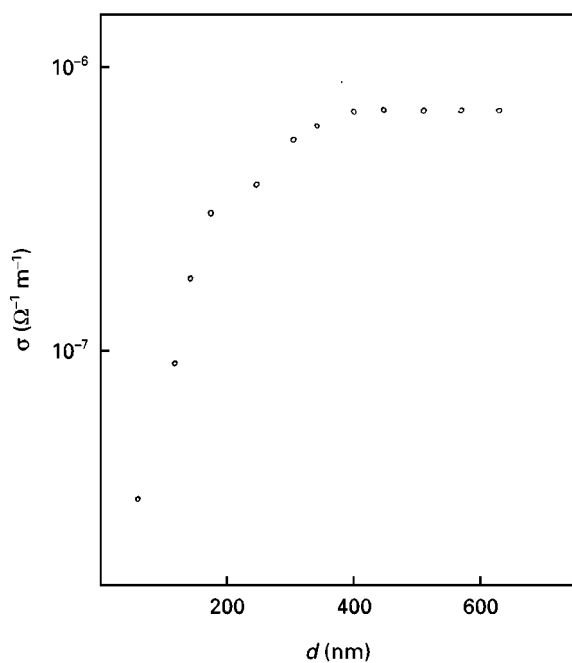


Figure 6 Thickness dependence of electrical conductivity for the as-deposited  $\text{In}_2\text{Te}_3$  films.

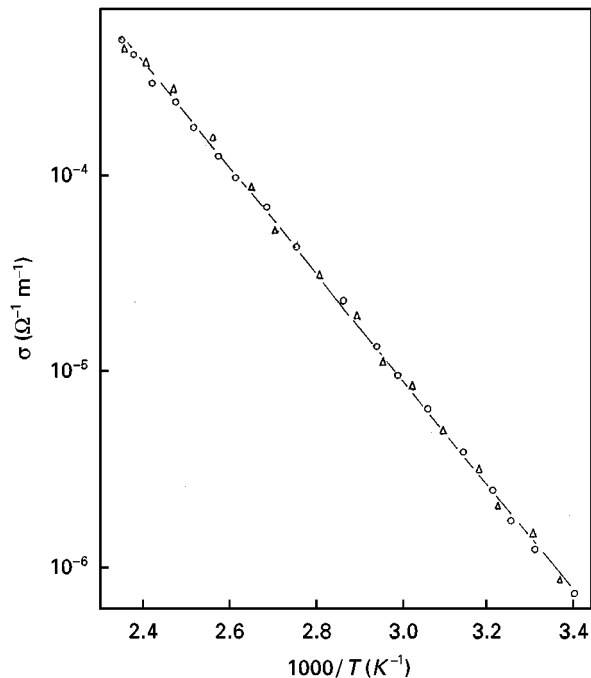


Figure 7 Temperature dependence of electrical conductivity for the as-deposited  $\text{In}_2\text{Te}_3$  film, 492 nm thick, during (○) heating and (△) cooling cycles.

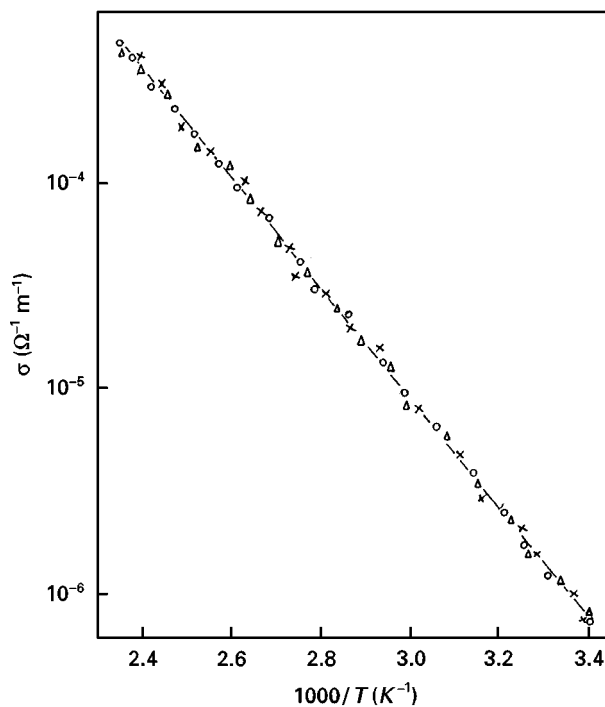


Figure 8 Temperature dependence of electrical conductivity for the as-deposited  $\text{In}_2\text{Te}_3$  films of different thicknesses: (○) 392 nm, (△) 490 nm, (×) 620 nm.

of the same thickness were annealed, each at one of the temperature values 423, 473, 523 and 573 K for 15 min, then for 30 min several times. The electrical conductivity,  $\sigma$ , was measured for the as-deposited samples, then after each annealing time until  $\sigma$  became stable, indicating the stability of the structure of the investigated film sample. This procedure was repeated for different samples in the investigated thickness range (322–620 nm) of the investigated composition. As

a representative example, the obtained data for the variation of  $\sigma_{RT}$  with the annealing times is given in Fig. 9 for samples of the same thickness (461 nm). It is clear that there is no distinguishable change in  $\sigma_{RT}$  for films annealed at 423 K in comparison with that of the as-deposited films. This means that annealing at

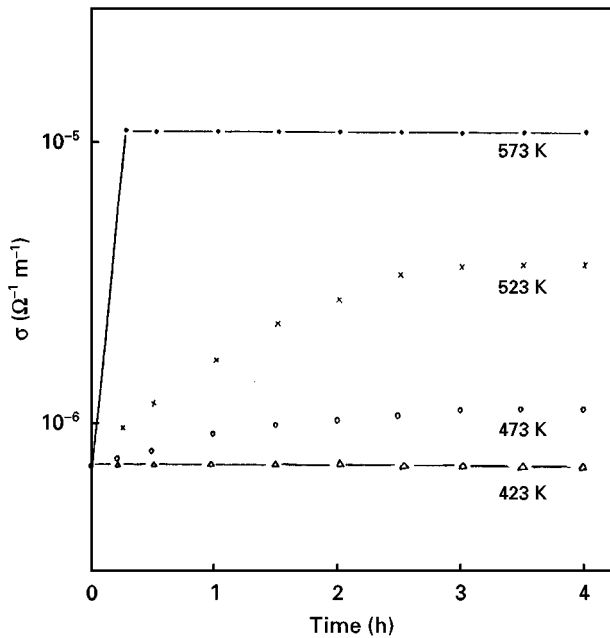


Figure 9 Effect of annealing on the electrical conductivity of  $\text{In}_2\text{Te}_3$  film, 461 nm thick.

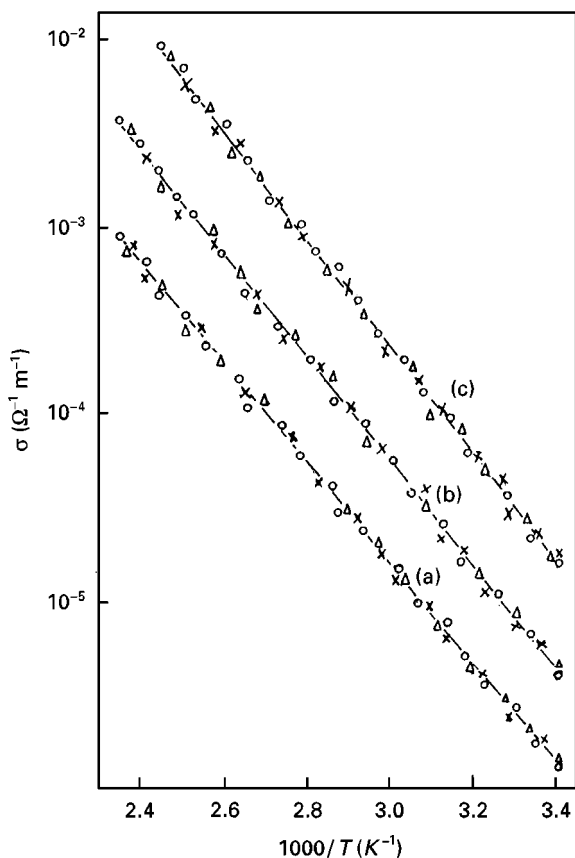


Figure 10 Temperature dependence of electrical conductivity for the  $\text{In}_2\text{Te}_3$  films annealed at (a) 473 K, (b) 523 K, (c) 573 K. (○) 392 nm, (△) 490 nm, (×) 620 nm.

a temperature less than  $T_g$  (443 K) does not affect the structure of the material. However,  $\text{In}_2\text{Te}_3$  films annealed at 473 and 523 K show an exponential increase in  $\sigma_{RT}$ , while those annealed at 573 K show an abrupt increase in  $\sigma_{RT}$  during the first 0.25 h, after which they remain constant with repeated annealing.

The variation of electrical conductivity with temperature of the above-mentioned annealed films was also measured, and the results are shown in Fig. 10 for samples annealed at 473, 523 and 573 K. The corresponding values of  $\Delta E_\sigma$  are 0.538, 0.564 and 0.582 eV, respectively. The observed increase in  $\Delta E_\sigma$  with increasing annealing temperature is in good agreement with the increase obtained before [17] in the optical energy gap which was explained on the basis of the theory proposed by Mott and Davis [18] for amorphous material. The presence of a high concentration of localized states in the band structure is responsible for the low value of  $E_g^{\text{opt}}$  and, consequently,  $\Delta E_\sigma$  in the case of the as-deposited amorphous films. In the process of heat treatment, the unsaturated defects are gradually annealed out [19] producing a larger number of saturated bonds. The reduction in the number of unsaturated defects decreases the density of localized states in the band structure and consequently increases the optical gap, and hence  $\Delta E_\sigma$  increases.

## References

1. E. G. GROCHOWSKI, D. R. MASON, G. A. SCHMITT and P. H. SMITH, *J. Phys. Chem. Solids* **25** (1964) 551.
2. S. A. HUSSEIN and A. T. NAGAT, *Phys. Status Solidi (a)* **114** (1989) K205.
3. A. A. ZAHAB, M. ABD-LEFDIL and M. CADENE, *ibid.* **115** (1989) 491.
4. V. A. PETRUSEVICH and V. M. SERGEEVA, *Sov. Phys. Solid State* **2** (1961) 2562.
5. A. A. ZAHAB, M. ABD-LEFDIL and M. CADENE, *Phys. Status Solidi (a)* **117** (1990) K103.
6. S. SEN and D. N. BOSE, *Solid State Commun.* **50** (1984) 39.
7. A. I. ZASLAVSKII and V. M. SEREGEEVA, *Sov. Phys. Solid State* **2** (1961) 2556.
8. G. L. BLERIS, T. KARAKOSTAS, J. STOEMENOS and N. A. ECONOMOU, *Phys. Status Solidi (a)* **34** (1976) 243.
9. T. KARAKOSTAS and N. A. ECONOMOU, *ibid.* **31** (1975) 89.
10. A. I. ZASLAVSKII, N. F. KARETNKO and Z. A. KARACHENTSEVA, *Sov. Phys. Solid State* **13** (1972) 2152.
11. G. L. BLERIS, TH. KARAKOSTAS, N. A. ECONOMOU and R. DE. RIDDER, *Phys. Status Solidi (a)* **50** (1978) 579.
12. V. M. KOSEVICH, A. A. SOKOL and A. D. BARVINOK, *Sov. Phys. Crystall.* **20** (1984) 212.
13. D. P. SINGH and K. D. KUNDRA, *J. Mater. Sci. Lett.* **8** (1989) 524.
14. S. TOLANSKY, "Introduction to interferometry" (Longmann, 1955).
15. I. YU. VERKELIS, *Sov. Phys. Solid State* **14** (1972) 1445.
16. A. G. KUNJOMANA and E. MATHAI, *J. Mater. Sci. Lett.* **11** (1992) 613.
17. N. A. HEGAB, A. E. BEKHEET, M. A. AFIFI and A. E. EL-SHAZLY, *J. Appl. Phys.*, to be published.
18. N. F. MOTT and E. A. DAVIS, *Electronic processes in non-crystalline materials* (Clarendon, Oxford, 1971).
19. S. HASEGAWA, S. YAZALCI and T. SHIMIZU, *Solid State Commun.* **26** (1978) 407.

Received 23 September 1996  
and accepted 27 January 1997